Effect of CsBr–$MnCl_2$ Mixed Fillers on the Crystal Structure and Optical and Electrical Properties of Poly(vinyl alcohol)

M. Abdelaziz

Department of Physics, Faculty of Science, Mansoura University 35516, P.O. Box 19, Mansoura, Egypt

Received 24 February 2004; accepted 8 July 2004
DOI 10.1002/app.21164
Published online in Wiley InterScience (www.interscience.wiley.com).

ABSTRACT: Poly(vinyl alcohol) (PVA) films filled with $(x)CsBr(15 - x)MnCl_2$, where $0.0 \leq x \leq 15\%$, were prepared by a casting technique. The crystal structure properties of the prepared films were examined by XRD, DTA, and FTIR. A correlation between XRD, DTA, and FTIR of the filled polymer was discussed. Optical absorption measurements revealed two optical band gaps (E_{g1} and E_{g2}). The electrical properties were studied using dc electrical conductivity. The filling level (FL) dependency of E_{g1} and E_{g2}, thermal activation energy (ΔE), and hopping distance (R_0) are given to illustrate the behavior of the filled polymers. © 2004 Wiley Periodicals, Inc. J Appl Polym Sci 94: 2178–2186, 2004

Key words: poly(vinyl alcohol); additives; crystal structures; UV–vis spectroscopy; activation energy

INTRODUCTION

Polymeric systems containing small metal particles are attractive systems because they are expected to exhibit properties that are of both scientific and practical interest. The formation of stable metal particles inside the polymer systems is important for many applications, such as three-dimensional (3D) storage of optical data, shielding of electromagnetic radiation,[1] and both pharmaceutical and medical fields.[2]

Poly(vinyl alcohol) (PVA) is a nontoxic water-soluble synthetic polymer, which is widely used in biochemical and medical applications because of its compatibility with the living body.[3] PVA has good film-forming and highly hydrophilic properties, and has been studied as a membrane in various ways. PVA has recently been exploited as a substrate for enzyme immobilization in the form of photo crosslinkable PVA.[4]

Manganese is well known as a magnetoactive multivalent element; thus its halides can be used as fillers to modify the electric conduction and the optical absorption of PVA. On the other hand, $MnCl_2$ is considered a good candidate for one- or two-dimensional phenomena[5] and for optical memory devices.[6]

In previous work, our research group investigated the physical properties of PVA films filled with $MnCl_2$.[7] It was revealed that the used filler modified the structural, optical absorption, and electric properties of PVA. However, a nonlinear and even non-monotonic filling level (FL) dependency of the contents of the active structural forms was found. Seeking for a linear or monotonic FL dependency of the optical absorption and electrical properties, we chose to use the intrasubstituted mixed fillers of CsBr and $MnCl_2$.

In the present work, we continue our effort to study the effect of the two mixed fillers on the physical properties of PVA. XRD, DTA, and FTIR were used to investigate the crystal structure of PVA films.

EXPERIMENTAL

Preparation of samples

The studied films were prepared by the casting technique. Poly(vinyl alcohol) (PVA), of molecular weight M_w = 72,000, was provided by Merck (Darmstadt, Germany). CsBr and $MnCl_2$ were supplied by Aldrich Chemical Co. (Milwaukean, WI). Specified amounts of PVA, CsBr, and $MnCl_2$ were dissolved in distilled water. The solution, having the proper mass fraction, $(x)CsBr(15 - x)MnCl_2$, was added to the polymer at a suitable viscosity. A mixture of the solution was cast onto a clean glass plate and dried in an oven at 323 K for 1 week. The prepared films were kept in a dry atmosphere for 3 weeks to remove the solvent traces. PVA films with different mass fractions, $(x)CsBr(15 - x)MnCl_2$, were prepared, where x = 0.0, 1.0, 5.0, 7.5, 10, 14, and 15 wt %. The thickness of the films was in the range of 100 to 140 μm.

Physical measurements

X-ray diffraction (XRD) patterns were obtained using a Siemens (South Iselin, NJ) type F diffractometer with

Cu–K_α radiation and LiF monochromator. Differential thermal analysis (DTA) was carried out using a Shimadzu (Kyoto, Japan) DTA-50 apparatus, with measuring temperature in the range 30–300°C and a heating rate of 5°C/min. The IR spectrophotometer (PE 883, Perkin Elmer Cetus Instruments, Norwalk, CT) was used for measuring the IR spectra in the wavenumber range of 2700–200 cm^{-1}. UV–vis absorption spectra were measured in the wavelength range of 200–900 nm using a spectrometer (Perkin–Elmer UV–vis). The dc electrical resistivity was measured using an autorange multimeter (Keithley 175, Keithley Metrabyte, Taunton, MA) with an accuracy of ±0.2%.

RESULTS AND DISCUSSION

X-ray diffraction

XRD patterns of the filled PVA are shown in Figure 1. The observed spectra characterize a semicrystalline polymer possessing crystalline peaks at a scattering angle ($19° \leq 2\theta \leq 20°$) corresponding to a (101) and/or ($10\bar{1}$) spacing.[8] The intensity of the (101) peak can be taken as a measure of the degree of crystallinity (h) and plotted as a function of the filling level (FL), as shown in Figure 2. It is clear that the h exhibits a minimum at $x = 1\%$ and a maximum at $x = 7.5\%$.

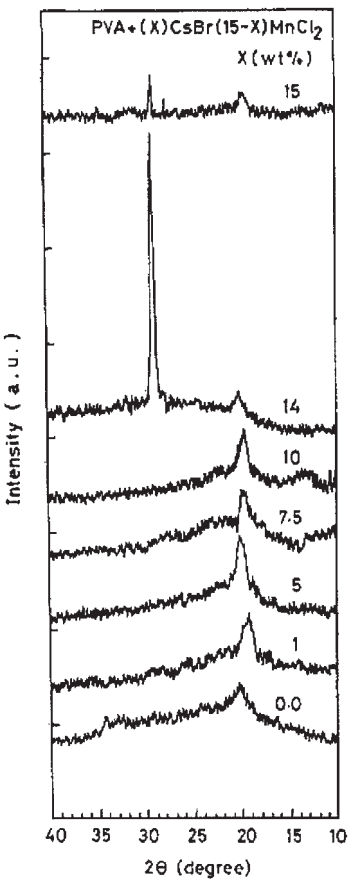

Figure 1 X-ray diffraction patterns of PVA films filled with $(x)CsBr(15 - x)MnCl_2$.

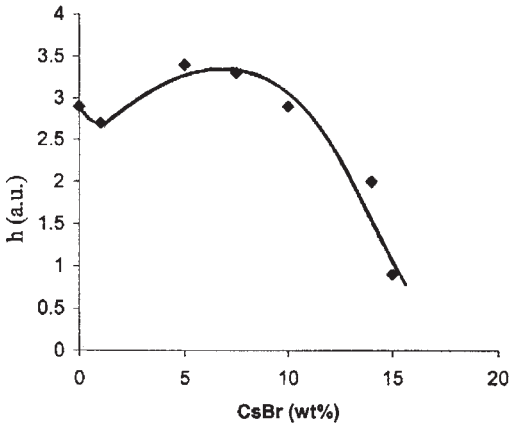

Figure 2 Filling-level (FL) dependency on the degree of crystallinity.

It is remarkable in Figure 1 that there is a sharp scattering peak at $2\theta \cong 30°$, for $x = 14$ and 15%. This peak is not attributed to PVA, CsBr, or $MnCl_2$ crystals. However, this peak may indicates the appearance of a new crystalline phase of the filled samples.[9]

The present results imply that the XRD profile is substantially influenced by the FL.

DTA thermograms

The DTA thermogram scans for PVA filled with $(x)CsBr(15 - x)MnCl_2$ are shown in Figure 3. All samples under study show two endothermic peaks in addition to one exothermic peak. These transitions can be interpreted as follows: the glass-transition temperature (T_g) of filled PVA was found to be around 35°C, which agrees with that reported in the literature.[10] The DTA scans of the filled PVA show a semicrystalline structure with the appearance of an exothermic peak at about 95°C, corresponding to the crystallization temperature (T_c).[11] The endothermic peak at about 206°C was attributed to the melting point (T_{m1}) of PVA.[8] Moreover, for $1 < x \leq 15\%$, there is another endothermic peak at about 225°C, indicating another melting point (T_{m2}) of the filled samples. According to the derivative DTA curves, the filled PVA films were found to degrade at a T_d of about 270°C.[10] The values of T_g, T_c, T_{m1}, T_{m2}, and T_d are detailed in Table I.

It is observed from Figure 3 and Table I that the position of T_g for PVA films filled with CsBr–$MnCl_2$ mixed fillers is shifted toward lower temperatures compared with that of the pure PVA.[12] This suggests that the segmental mobility of an amorphous pure PVA increases as a result of the addition of mixed fillers, becoming less-rigid segments. This indicates that the mixed fillers CsBr and $MnCl_2$ act as plasticizers. The change in position of T_c may be mainly attrib-

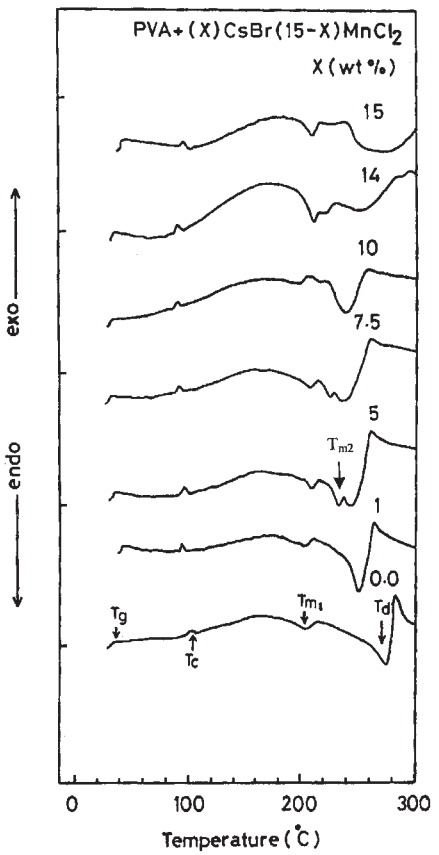

Figure 3 DTA thermograms of PVA films filled with mixed fillers.

utable to the effect of filling on the orientation of the crystals, crystallinity, and microstructure of the sample. They expect that T_c could be influenced by the size and perfection of the crystals and thus their melting point. On the other hand, Popli et al.[13] reported that T_c depends on the crystal thickness. Also, the magnitude of thermal degradation temperature (T_d) of the pure PVA[14] is greater than that of the filled samples. It is suggested that the addition of the mixed fillers to PVA films decreases the thermal stability.

Furthermore, it is interesting to find the appearance of two distinct T_m peaks for $1 < x \leq 15\%$ samples, as shown in Figure 3 and Table I. This implies that two crystalline phases, such as a syndiotactic sequence and an atactic sequence, may exist after incorporation of the mixed fillers into the PVA. This result confirmed the findings reported by Yeh et al.[12]

The variation of T_m of PVA crystals is evident with the variation of the FLs. The distribution of melting temperatures was converted to a distribution of crystalline thickness using the Thomson–Gibbs's equation[15]

$$T_m = T_m^\circ[1 - 2\sigma_e/\Delta HL] \quad (1)$$

where T_m is the observed melting temperature of a crystal of lamellar thickness L, T_m° is the equilibrium melting temperature of an infinitely thick crystal, σ_e is the surface area of the chain folds, and ΔH is the heat of fusion per unit volume of crystals. The value of $\sigma_e/\Delta H$ used for PVA was 3.3×10^{-8} cm and $T_m^\circ = 501.5$ K.[16] The calculated values of the crystal lamellar thickness are listed in Table I. It may be observed that the crystal lamellar thickness is influenced by the FLs.

IR spectroscopy

The infrared spectral analysis of the samples was performed over the range of 2700–200 cm^{-1}. Figure 4 shows the absorption spectra for the filled PVA with two mixed fillers. A slight variation was observed in the absorption bands of the filled PVA compared with that previously reported for pure PVA.[17] The assignment of these bands for all samples under study is given in Table II.

By using the ratio I_{sy} of the peaks at 942 and 830 cm^{-1} as a measure for the syndiotacticity of the PVA,[18] additional characteristics of the samples may be shown by plotting the FL dependency of I_{sy}, as shown in Figure 5. It is to be noticed that the syndio-

TABLE I
FL Dependency of Glass Transition; Crystallization (T_c), Melting (T_m), and Degradation (T_d) Temperatures; and Crystalline Lamellar Thickness (L)

CsBr (wt %)	T_g (°C)	T_c (°C)	T_{m1} (°C)	T_{m2} (°C)	T_d (°C)	L (Å)
Unfilled	50	109.0	226.5	—	326.0	1655
0.0	35	104.67	206.27	—	275.07	148.9
1	43	96.76	205.63	—	252.42	144.4
5	35	95.29	209.39	233.33	232.68	173.0
7.5	35	92.82	209.21	225.92	239.16	171.6
10	45	98.26	206.00	216.66	244.55	147.0
14	35	89.54	210.86	222.22	250.50	187.0
15	45	95.16	210.42	225.92	270.17	183.0

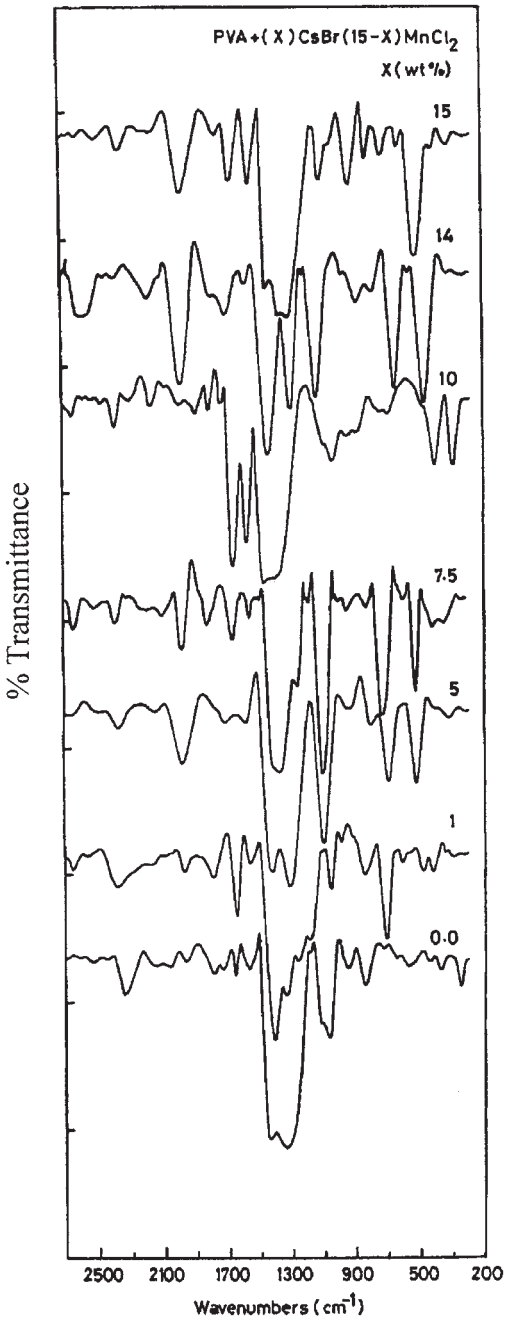

Figure 4 FTIR spectra of PVA films filled with mixed fillers.

tacticity changes slightly and monotonically, whereas a minimum syndiotacticity was observed at $x = 5\%$. Naguro et al.[19] reported that the increase in the syndiotacticity of PVA samples causes dense molecular packing in the crystal and also stronger intermolecular hydrogen bonds, which are responsible for the disappearance of the molecular motion.

Moreover, the ratio I_{OH} of the intensity of the peaks at 1339 and 1438 cm^{-1} may be used as a measure of the OH mode of deformation attributed to the mixed fillers.[7] The FL dependency of I_{OH} is shown in Figure 5. This indicates that the CsBr–$MnCl_2$ mixed fillers

TABLE II
Assignments of the IR Characterizing Peaks of the PVA System[a]

Frequency (cm^{-1})	Assignment
830	ν(CC)
942	$\nu(CH_2)$
1107	ν(CO)
1339	δ(CH + OH)
1438	CH_2 bending
1565	O—H and C—H bending
1660	Absorbed H_2O
1791	ν(C═O)

[a] From Rabie et al.[17]

affect the bending mode of the OH group of PVA. This result confirmed findings previously obtained for the $MnCl_2$ filled PVA,[7] in which the OH bending mode was substantially affected by the FL of $MnCl_2$.

The percentage crystallinity of the samples was determined by using the following relation[20]:

$$\text{Percentage crystallinity} = 92(d/c) - 18 \quad (2)$$

where d is the absorbance of the 1100 cm^{-1} peak and c is the absorbance of the 1420 cm^{-1} peak. The absorbance was measured by using the baseline method. The FL dependency of the percentage crystallinity is shown in Figure 6. It is clear that the percentage crystallinity exhibits a minimum value at $x = 1\%$ and a maximum value at $x = 7.5\%$.

The FL dependencies of the intensity of the peaks at 570 cm^{-1}, which was assigned to C—Br vibrating mode,[18] and 1339 cm^{-1}, which was assigned to O—H and C—H bending,[21] are plotted in Figure 7. Each exhibits two minima at $x = 1$ and 14% and maximum

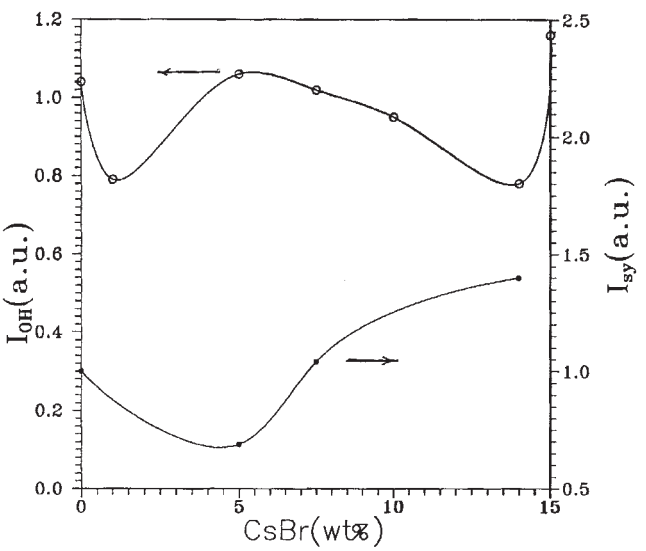

Figure 5 FL dependency of the I_{sy}, representing the syndiotactic ratio, and I_{OH}, representing the OH bending mode.

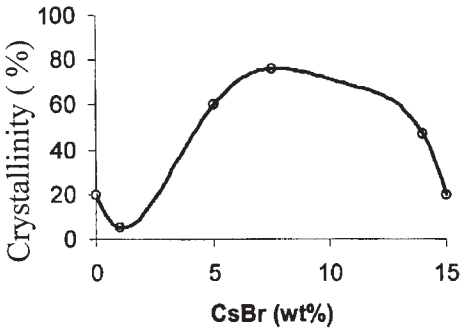

Figure 6 FL dependency of the percentage crystallinity of the filled PVA films.

at $x = 7.5\%$, indicating different modes of structural deformation. It seems important to obtain more insight about the other physical properties of PVA films filled with CsBr–$MnCl_2$ mixed fillers.

Optical absorption spectra

Figure 8 shows the optical absorption spectra of PVA filled with mixed fillers CsBr and $MnCl_2$. One may divide these spectra into two regions according to the wavelength.

The ultraviolet region (UV)

In the UV region of Figure 8, we reported that all the samples show two absorption bands at nearly the same position (277 and 323 nm). Among these observed bands, the band at 277 nm arising from $(CH_3)_2C{=}O$,[22] is attributed to the electronic transition[23]

$$^4A_{2g} \rightarrow {}^4T_{1g}(P) \tag{3}$$

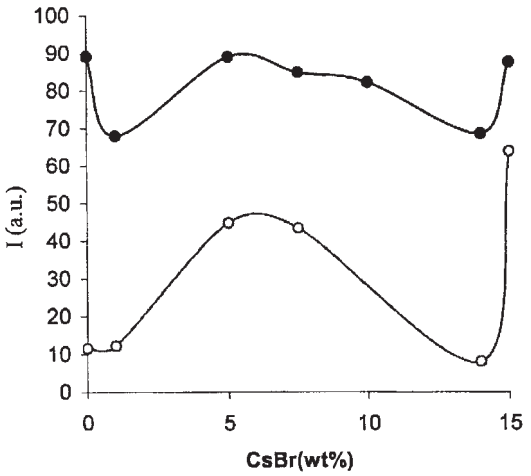

Figure 7 FL dependency of the absorption peaks at (●) 1339 and (○) 570 cm^{-1}.

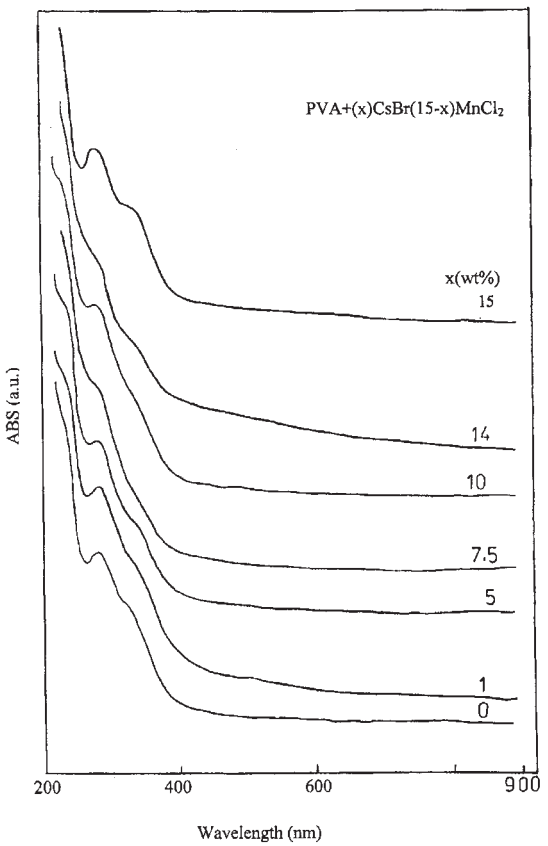

Figure 8 UV–vis spectra of PVA films filled with $(x)CsBr(15 - x)MnCl_2$.

whereas the weak shoulder at 323 nm is attributed to the $-C(CH{=}CH)_3CO$ structure.[24] In other words, the bands that appeared at 277 and 323 nm, with different absorption intensities, may be assigned to π–π^*, which comes from unsaturated bonds, mainly C═O and/or C═C, which are present in the tail–head of the polymer.[25]

The visible region

The variation of optical absorption with wavelength (λ) for all the samples is shown in Figure 8. The recorded optical data were analyzed for both possible allowed and forbidden optical transitions. The optical data were analyzed from the classical relation for near-edge optical absorption in semiconductors[26]

$$\alpha h\upsilon = A[(h\nu - E_g)^n] \tag{4}$$

where α is the linear absorption coefficient, which was calculated using the following equation[27]:

$$\alpha(\nu) = \ln[t_1(\nu)/t_2(\nu)]/(d_2 - d_1) \tag{5}$$

where $t_1(\nu)$ and $t_2(\nu)$ are the transmittances of two films (of the same FL) with thickness d_1 and d_2, ν is the

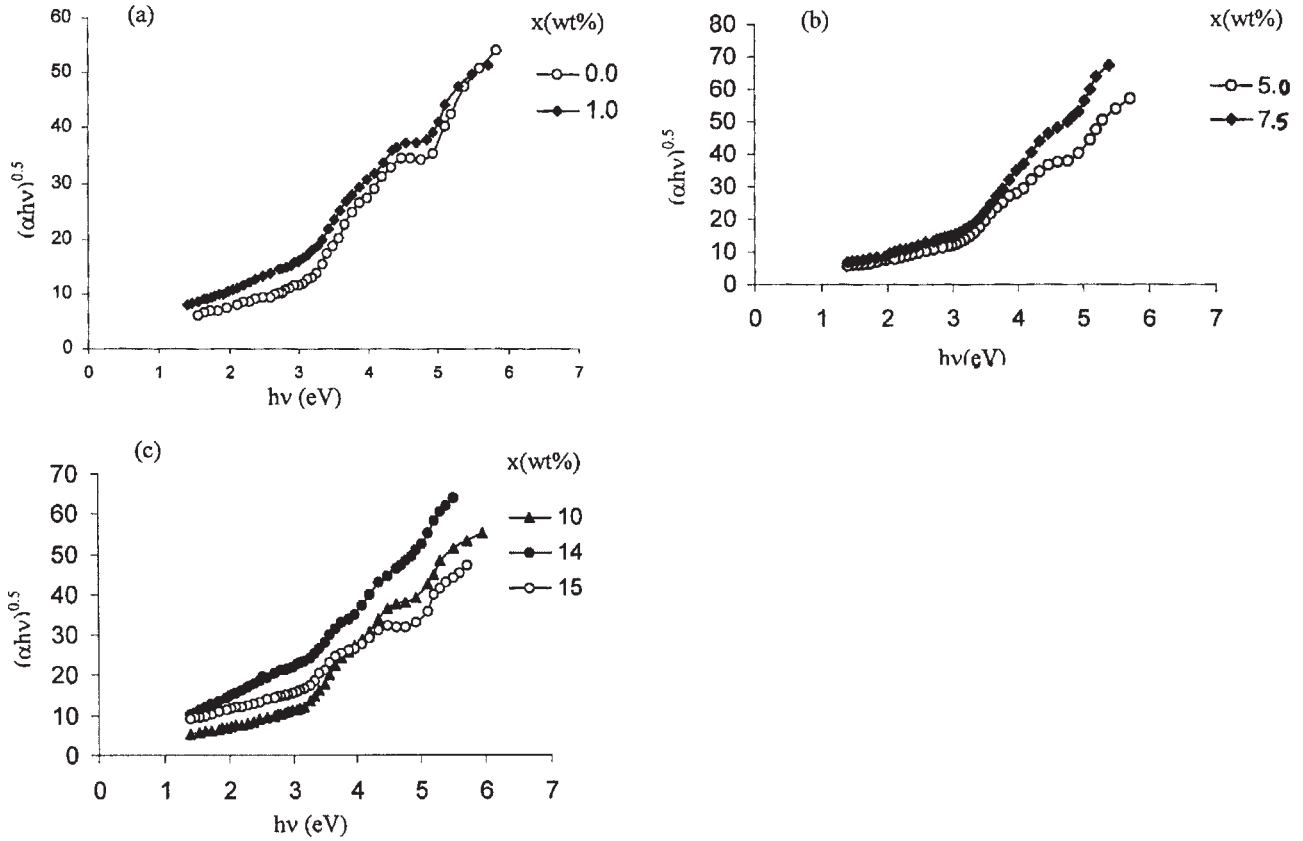

Figure 9 Product of optical absorption coefficient and photon energy versus the photon energy $h\nu$.

frequency, h is Plank's constant, and n depends on the kind of optical transition that prevails. Specifically, n is 1/2, 3/2, 2, and 3 for transitions designated as direct allowed, direct forbidden, indirect allowed, and indirect forbidden, respectively. A is a constant and E_g is defined as the energy band gap between the valence band and the conduction band. We plotted the $(\alpha h\nu)^{1/2}$ versus photon energy ($h\nu$) using the absorption spectra data of these samples. The plots of $(\alpha h\nu)^{1/2}$ versus $h\nu$ give two linear portions, as shown in Figure 9(a)–(c). The optical band gaps of all samples were determined and are shown in Figure 10. The linear extrapolations yield the optical energy band gaps E_g. Figure 10 displays the dependency of the two optical gaps on the CsBr content. It is clear that E_{g1} and E_{g2} exhibit maximum values at x = 7.5% and minimum values at x = 1%. It is remarkable that these concentrations, minimum at x = 1% and maximum at x = 7.5%, were in agreement with the crystallinity results obtained from XRD (see Fig. 2) and IR absorption peaks (see Fig. 6). This indicates that the optical energy gaps are significantly influenced by the crystal structure.

Dc conductivity

The dc electrical resistivity (ρ) of the samples was measured in the temperature range of room temperature to 400 K. The temperature dependency of the electrical resistivity was examined according to two basic existing theories: the Arrhenius model and modified interpolaron-hopping model. The obtained results can be concluded as follows.

Arrhenius behavior is observed in the range of 333 to 388 K [see Fig. 11(a)–(c)]. The resistivity data may be fitted to straight lines, where resistvity can be analyzed by an Arrhenius equation of the form

$$\rho = \rho_0 \exp(\Delta E/KT) \tag{6}$$

where ρ_0 is the preexponential factor and ΔE is the thermal activation energy for conduction. The values

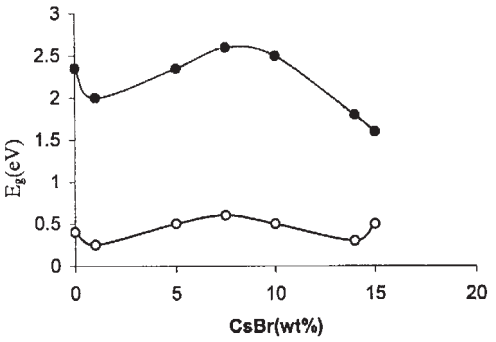

Figure 10 FL dependency of the optical energy gaps (○) E_{g1} and (●) E_{g2}.

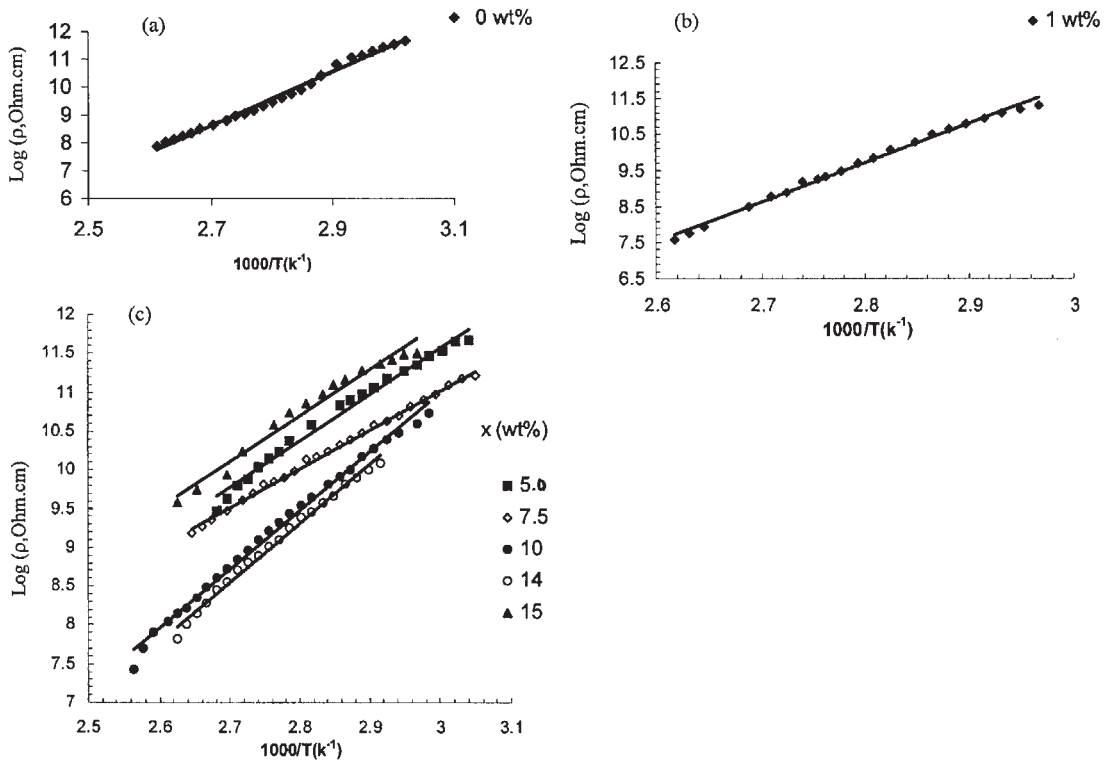

Figure 11 Temperature dependency of the logarithm of electrical resistivity for various filling levels.

of ΔE were determined and are shown in Figure 12. The activation energies may correspond to the different energy levels. The values of activation energies are related to the intramolecular conduction process.[28] It is remarkable that the FL dependency of ΔE is nearly similar in behavior to the FL dependency of the reciprocal crystallinity (detected by XRD and IR analysis). This indicates that the conduction mechanism was influenced by an amorphous domain. It is known that the electrical conductivity of polymeric films is attributed to transport of the charge carriers in the polymeric matrix. The ionic mobility is increased by segmental motion of the PVA polymer, where the ionic conductivity is mainly localized to the amorphous phase. The increase of conductivity with temperature is explained as being the result of a hopping mechanism between coordinate sites, local structural relaxation, and segmental motions of the polymer. Segmental motion more readily occurs in the amorphous phase of PVA polymer matrix.

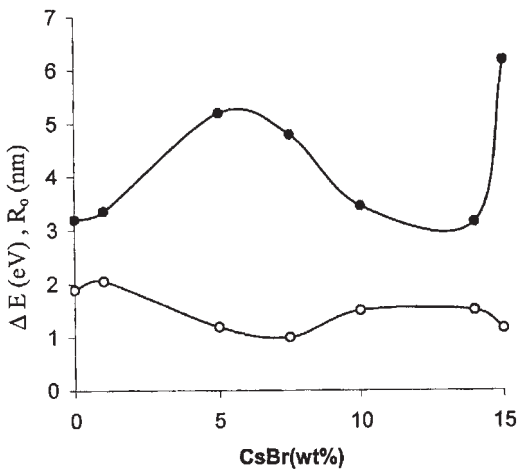

Figure 12 FL dependency of thermal activation energy (○) ΔE and hopping distance (●) R_0.

It is known that double-bond segments and structural defects (detected by IR spectroscopy and optical absorption measurements) are considered as suitable sites for the formation of polarons and/or bipolarons in the polymeric matrix. Therefore, the electrical resistivity can be expressed by

$$\rho = \frac{kT}{Ae^2\gamma(T)^2}\frac{R_0^2}{\xi}\frac{(y_p + y_{bp})^2}{y_p y_{bp}}\exp\left(\frac{2BR_0}{\xi}\right) \qquad (7)$$

where $A = 0.45$; $B = 1.39$; y_p and y_{bp} are the concentration of polarons and bipolarons, respectively; R_0 is the typical separation between impurities; $\zeta = (\zeta_\parallel \zeta_\perp^2)^{1/3}$ is the average decay length of a polaron and bipolaron wave function; $\zeta_\parallel$ and $\zeta_\perp$ are the decay lengths parallel and perpendicular to the polymer chain, respectively. Bredas et al.[29] reported that the extension of defect should be the same for both polarons and bipolarons. The electronic transition rate

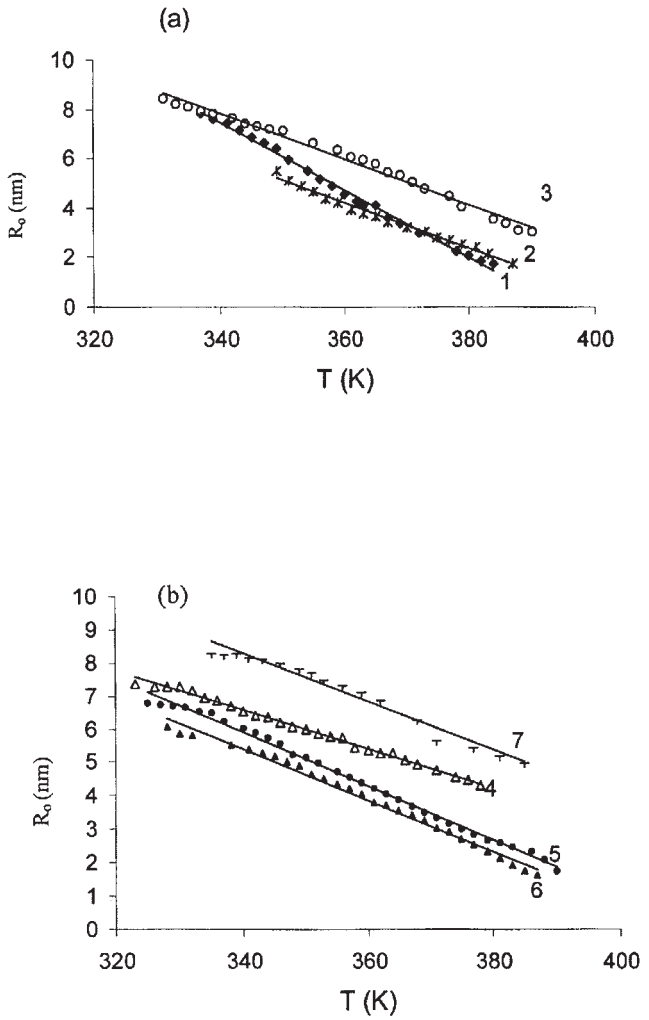

Figure 13 Temperature dependency of the hopping distances for various filling levels (in wt %): (a) curve 1: 0.0; curve 2: 1; curve 3: 5; (b) curve 4: 7.5; curve 5: 10; curve 6: 14; curve 7: 15.

between polaron and bipolaron states can be expressed as

$$\gamma(T) = 1.2 \times 10^{17}(T/300\ K)^{11} \quad (8)$$

Using a computer-aided program, the order of magnitude of ρ in the present system was adjusted with the impurity concentration, which actually was the fitting parameter. The parameter $\zeta_{\|} = 1.06$ nm, whereas $\zeta_{\perp} = 0.22$ nm,[30] which depends on the interchain resonance energy and the interchain distance. Taking $y_p = y_{bp}$ for simplicity, which is an acceptable approximation,[31] using eqs. (7) and (8), we can obtain the values of the hopping distance R_0. A linear decrease of R_0 as the temperature increases, for various FLs, is observed in Figure 13. This indicates that the concentration of thermally activated polarons (acting as hopping sites for the charge carriers) increases gradually as the temperature increases.

Figure 12 shows the FL dependency of calculated R_0 at $T = 370$ K. It is clear that R_0 exhibits a maximum at $x = 5\%$ and a minimum at $x = 14\%$, representing the mirror image of the corresponding dependency of the peaks at 570 and 1339 cm^{-1} and I_{OH} (see Figs. 5 and 7). This indicates that the hopping-conduction mechanism is affected by these localized states; Br, O—H, and C—H bending; and deformation type of the OH mode.

CONCLUSIONS

In this work, PVA films filled with (x)CsBr$(15 - x)MnCl_2$ were obtained by a cast method. The structural modifications of the prepared samples were studied by using XRD, DTA, and IR spectroscopy. XRD and DTA revealed the appearance of another crystalline phase beside the original PVA crystalline phase. Some physical quantities, such as optical energy gaps, thermal activation energy and hopping distance, were determined. The changes in the values of these physical quantities under different FLs were correlated with the crystal structure. The present of CsBr–$MnCl_2$-filled PVA system is good candidate for one-dimensional technical (optical and/or electric) applications.

References

1. Mc Phail, D.; Gu, M. Appl Phys Lett 2002, 18, 1160.
2. Oster, J.; Parker, J.; Brassard, L. J Magn Magn Mater 2001, 225, 145.
3. Yamamura, K.; Kuranuki, N.; Suzuki, M.; Tanigami, T.; Matsuzawa, S. J Appl Polym Sci 1990, 41, 2409.
4. Pattanapipitpaisal, P.; Brown, N. L.; Macaskie, L. E. Biotechnol Lett 2001, 23, 61.
5. Tawansi, A.; Oraby, A. H.; Abdelrazek, E. M.; Ayad, M. I.; Abdelaziz, M. J Appl Polym Sci 1998, 70, 1437.
6. Zhang, Q.; Whatmore, R. W. J Phys D: Appl Phys 2001, 34, 2296.
7. Tawansi, A.; Oraby, A. H.; Zidan, H. M.; Dorgham, M. E. Physica B 1998, 254, 126.
8. Strawhecker, K. E.; Manias, E. Chem Mater 2000, 12, 2943.
9. Fahmy, T. Int J Polym Mater 2001, 50, 109.
10. Peesan, M.; Rujiravanit, R.; Supaphal, P. Polym Test 2003, 22, 381.
11. Jong, J.; Lee, D. Polymer 2003, 44, 8139, 69.
12. Yu, Y.-H.; Lin, C.-Y.; Yech, J.-M.; Lin, W.-H. Polymer 2003, 44, 3553.
13. Popli, R.; Glotin, M.; Mandelkern, L.; Benson, R. S. J Polym Sci Part B: Polym Phys 1984, 22, 407.
14. Zidan, H. M. J Appl Polym Sci 2003, 88, 1115.
15. Gibbs, J. H. Collected Works; Longman Green: Essex, UK, 1982.
16. Mallaprogada, S. K.; Peppas, N. A. J Polym Sci Part B: Polym Phys 1996, 34, 1339.
17. Rabie, S. M.; Abdel-Hakeem, N.; Moharram, M. A. J Appl Polym Sci 1989, 38, 2269.

18. Tawansi, A.; Zidan, H. M.; Oraby, A. H.; Dorgham, M. E. J Phys D: Appl Phys 1998, 31, 3429.
19. Nagura, M.; Matsuzawa, S.; Yamamura, K.; Ishikawa, H. Polym J 1982, 14, 69.
20. Hokarram, M. A.; Robie, S. M.; El-Hamouly, W. S. J Appl Polym Sci 1991, 42, 3025.
21. Ibrahim, A. J.; Attia, G.; Abo-Ellil, M. S.; Abd El-Kader, F. H. J Appl Polym Sci 1997, 63, 343.
22. Rao, N. R. Ultraviolet and Visible Spectroscopy: Chemical Applications; Butterworth: London, 1967.
23. Abd El-Kader, F. H.; Hamza, S. S.; Attia, G. J Mater Sci 1993, 28, 6719.
24. Zidan, H. M. Polym Test 1999, 18, 449.
25. Abd El-Kader, K. A. M.; Abdel-Hamied, S. F.; Mansour, A. B.; El-Lawindy, A. M. Y.; El-Tantaway, F. Polym Test 2002, 21, 847.
26. Yakuphanoglu, F.; Erol, I.; Aydogdu, Y.; Ahmedzade, M. Mater Lett 2002, 57, 229.
27. Chiodlli, G.; Magistris, A. Solid State Ionics 1986, 18, 356.
28. Yakuphanoglu, F.; Aydogdu, Y.; Schatzschneider, U.; Rentscher, E. Physica B 2003, 334, 443.
29. Breads, J. L.; Chance, R. R.; Silbey, R. Phys Rev 1982, B26, 5843.
30. Mott, N. F.; Gurrey, R. W. Electronic Process in Ionic Crystals; Oxford University Press: London, 1940.
31. Tawansi, A.; Badr, S. I.; Abdelaziz, M. J Mater Design Appl 2002, 57.